NASA TECHNICAL NOTE

NASA TN D-7894

NASA TN D-7894

EFFECT OF ADSORBED CHLORINE AND OXYGEN ON SHEAR STRENGTH OF IRON AND COPPER JUNCTIONS

Donald R. Wheeler

Lewis Research Center

Cleveland, Ohio 44135

NATIONAL AERONAUTICS AND SPACE ADMINISTRATION • WASHINGTON, D. C. • JANUARY 1975

1. Report No.	2. Government Accession No.	3. Recipient's Catalog No.
NASA TN D-7894		

4. Title and Subtitle	5. Report Date
EFFECT OF ADSORBED CHLORINE AND OXYGEN ON SHEAR STRENGTH OF IRON AND COPPER JUNCTIONS	January 1975
	6. Performing Organization Code
7. Author(s)	8. Performing Organization Report No.
Donald R. Wheeler	E-8122
	10. Work Unit No.
9. Performing Organization Name and Address	506-16
Lewis Research Center National Aeronautics and Space Administration Cleveland, Ohio 44135	11. Contract or Grant No.
	13. Type of Report and Period Covered
12. Sponsoring Agency Name and Address	Technical Note
National Aeronautics and Space Administration Washington, D.C. 20546	14. Sponsoring Agency Code

15. Supplementary Notes

16. Abstract

Static friction experiments were performed in ultrahigh vacuum at room temperature on copper, iron, and steel contacts selectively contaminated with oxygen and chlorine in submonolayer amounts. The concentration of the adsorbates was determined with Auger electron spectroscopy and was measured relative to the saturation concentration of oxygen on iron (concentration 1.0). The coefficient of static friction decreased with increasing adsorbate concentration. It was independent of the metal and the adsorbate. The results compared satisfactorily with an extension of the junction growth theory to heterogeneous interfaces. The reduction in interfacial shear strength was measured by the ratio s_a/s_m, where s_a is the shear strength of the interface with an adsorbate concentration of 1.0, and s_m is the strength of the clean metal interface. This ratio was 0.835±0.012 for all the systems tested.

17. Key Words (Suggested by Author(s))

Adsorption
Static friction
Adhesion
Iron
Copper

18. Distribution Statement

Unclassified - unlimited
STAR category 37 (rev.)

19. Security Classif. (of this report)	20. Security Classif. (of this page)	21. No. of Pages	22. Price*
Unclassified	Unclassified	25	$3.00

* For sale by the National Technical Information Service, Springfield, Virginia 22151

EFFECT OF ADSORBED CHLORINE AND OXYGEN ON SHEAR STRENGTH OF IRON AND COPPER JUNCTIONS

by Donald R. Wheeler

Lewis Research Center

SUMMARY

Static friction experiments were performed in ultrahigh vacuum at room temperature on copper, iron, and steel contacts selectively contaminated with oxygen and chlorine in submonolayer amounts. The concentration of the adsorbates was determined with Auger electron spectroscopy and was measured relative to the saturation concentration of oxygen on iron (concentration 1.0). The coefficient of static friction decreased with increasing adsorbate concentration. It was independent of the metal and the adsorbate.

The results compared satisfactorily with an extension of the junction growth theory to heterogeneous interfaces. The reduction in interfacial shear strength was measured by the ratio s_a/s_m, where s_a is the shear strength of the interface with an adsorbate concentration of 1.0, and s_m is the strength of the clean metal interface. This ratio was 0.835±0.012 for all the systems tested.

INTRODUCTION

Extreme-pressure lubrication problems are characterized by high pressure or high temperature, which results in the extrusion or breakdown of conventional boundary lubricant films. Lubricant additives containing active phosphorus, sulfur, and chlorine are commonly used in these cases to reduce friction and wear. Oxygen, usually present naturally, is also recognized as effective in extreme-pressure lubrication. One explanation of extreme-pressure additive action is that, at the high temperatures existing at the metal interface, the atoms combine chemically with the metal to produce multiatomic-layer chemical films of low shear strength (ref. 1). These films then reduce friction and metal-metal contact. On the other hand, there is evidence that chemisorbed films less than a monolayer thick can also reduce metal friction (ref. 2). This is on a

much different scale than a chemical film and could be part of a different mechanism of additive action.

The purpose of the work described in this report was to examine the effect of chemisorbed oxygen and chlorine on the shear strength of copper, iron, and steel interfaces. The results were analyzed by using the junction growth theory of friction (ref. 3) in order to verify the theory, to find the functional relation between adsorbate coverage and friction, and to determine numerical values for the shear strengths of the systems studied. An attempt was made to duplicate extreme-pressure conditions while retaining complete control of the environment. Static friction experiments were conducted between atomically clean or contaminated metals in ultra-high-vacuum conditions. The contact areas and loads were such as to produce large plastic deformation of the asperity junctions. Auger electron spectroscopy was used to monitor the concentration of the contaminant.

SYMBOLS

A	real area of contact normal and tangential force
A_e	area of real contact according to Hertzian elastic theory
A_o	real area of contact under purely normal stress
c	adsorbate concentration in junction after junction growth (relative to saturation concentration of oxygen on iron)
c'	measured adsorbate concentration on undisturbed metal surface (relative to saturation concentration of oxygen on iron)
F	tangential force
k	s_i/s_m
p	normal stress, W/A
p_o	yield pressure of metal
s	tangential stress, F/A
s_i	specific shear strength of interfacial contaminant layer
s_m	specific shear strength of atomically clean metal
W	normal load
α	undetermined parameter of plasticity theory
μ	coefficient of friction

μ_s static coefficient of friction

φ maximum force coefficient, F/W

EXPERIMENT

Materials

The friction test specimens were 6.5-centimeter-diameter by 1.2-centimeter-thick disks contacted by hemispherical riders with a 0.476-centimeter radius. All specimens were ground to a fine finish on 600-grit metallurgical papers. The riders were then polished with 1-micrometer aluminum oxide powder. The disks were finished first with 6- and 3-micrometer diamond polish and then with 1-micrometer aluminum oxide. The disks were finally cleaned in the vacuum system by sputtering in an argon glow discharge. The disk was biased to 1000 volts negative, and the system was backfilled with argon until a discharge current of about 10 milliamperes was obtained.

A microhardness test was made on each disk with a Vickers diamond indenter at a 164-gram load. The load was chosen to be close to that used in the actual friction measurements. The copper disk was fabricated from zone-refined copper. It had a Vickers hardness number of 58.5±1.3 kilograms per square millimeter. The iron disk was 99.95 percent iron and had a Vickers hardness number of 79.6±1.0 kilograms per square millimeter. The steel disk was AISI 52100 bearing steel with a Vickers hardness number of 480±13 kilograms per square millimeter. In every case the rider was AISI 52100 bearing steel with a transfer layer of disk material, as explained in the next section.

The gases used were commercial grade oxygen and chlorine. Their purity in the vacuum chamber was measured with a quadrupole mass spectrometer. In all cases impurities were less than a few percent and were primarily hydrochloric acid for chlorine and water for oxygen. These impurities were probably formed from hydrogen that flowed out of the ion pump when the gases were admitted. Separate experiments showed that the adsorption rates for these impurities were less than those for the gases of interest. Later results showed that this level of impurity could have had no measurable effect on the friction.

Friction Measurements

The rider and disk specimens were mounted in the experimental vacuum chamber shown schematically in figure 1. The rider was deadweight loaded with 100 grams against the disk, which was positioned with the magnetic drive. The tangential force

was measured with a strain gage which was pulled uniformly by means of a motor drive attached to it. In the absence of any motion of the pin relative to the disk, the tangential force increased at a rate of about 3×10^{-2} newton per second (3×10^{3} dynes/sec). The displacement of the arm carrying the rider was measured with a capacitance probe in close proximity to a metal flat on the rider support arm. A bridge measured the change in capacitance produced by motion of the arm and produced a direct-current voltage proportional to this motion. An x, y-recorder was used to plot graphs of force as a function of motion. All experiments were performed at room temperature.

The procedure for each test was to move to an unused spot on the disk and lower the rider carefully to the disk. The rider was allowed to remain in contact with the disk for 1 minute before any tangential force was applied. Then the drive motor was turned on, and the friction trace was obtained on the x, y-recorder. The rider was raised, and the drive motor was reversed to its starting position. Before any reliable friction tests could be made, the procedure was repeated many times to assure that a layer of disk material was transferred to the rider, or when the steel disk was used, to assure that the rider was scoured clean of contaminants. In either case the maximum friction eventually stabilized at a high value. Microscopic examination of the tip of the rider after tests were completed verified the presence of the transferred copper. Thus, the contacts were always between like metals, and the metal on the rider was a thin, heavily cold-worked layer on a very hard steel substrate.

Some typical plots for copper on copper both with and without adsorbed chlorine are shown in figure 2. The external motion shown on the horizontal scale does not represent true relative motion of the pin and disk, because there was some motion due to yield of the gimbals and magnetic drive and flexing of the rider holder arm. As a result there was some apparent displacement for any applied force, even in the absence of motion of the rider relative to the disk (contact motion). The nature of this yielding was determined in separate experiments. With the pin clamped mechanically to the disk, a trace was produced that was nearly coincident with the friction traces up to a force coefficient of 1. Beyond that point increasing contact motion was evident.

The onset of sliding was not sudden, so that the choice of a static coefficient of friction for the bare metal was somewhat arbitrary. Only the maximum force coefficient achieved was of use. For contaminated metals the force coefficient at which the trace began to deviate from the clean metal trace was chosen as the static coefficient of friction since it best represented the influence of the contaminant in weakening the junction.

Auger Electron Spectroscopy

The surface of the disk could be examined by Auger electron spectroscopy (ref. 4) by using the cylindrical mirror analyzer shown in figure 1. A beam of electrons from

an electron gun in the analyzer was directed onto the disk surface, and the derivative of the energy spectrum of the secondary electrons was recorded. In these experiments the beam current was 5 microamperes, and the electrons had an energy of 2 kiloelectron volts. Two typical spectra are shown in figure 3. The energy of the negative peak of the derivative curve is conventionally chosen as the energy to be assigned to the peak. The energy, as well as the peak shape, is characteristic of the element it represents. Because of the low energies of the Auger electrons, this technique is sensitive only to the first few atomic layers. It is easy to detect fractional monolayer coverages of adsorbed species on the clean metal disks.

It was a matter of some importance to determine the relative amounts of different adsorbates on different metal surfaces. To do this, small samples of copper and iron were mounted in a disk so that they could be cleaned, exposed to an adsorbate, and analyzed without opening the vacuum system or disturbing the Auger analyzer in any way. As the exposure (defined as the product of adsorbate pressure and adsorption time) was increased, the Auger signal increased to a maximum value. This was apparently a saturation concentration of the adsorbate on the metal. The spectra of figure 3, for example, were taken under such conditions. The samples of copper and iron were given saturation exposures of chlorine and oxygen, and spectra were recorded for the exposed metals as well as for the clean metals.

The work of reference 5 showed that up to coverages of one monolayer the peak-to-peak height of the adsorbate Auger spectral line is proportional to the concentration in atoms per unit area of adsorbate on the surface. However, work reported in references 6 to 8 indicated that, at least on nickel, a saturation concentration of oxygen at room temperature consists of two atomic layers. This may also be true of iron. Reference 6, however, concludes that even at this concentration the error in taking the oxygen Auger peak-to-peak height to be proportional to the oxygen concentration is less than 14 percent. An error of that size was tolerable in this study, in view of other experimental uncertainties. Thus, we may conclude that, for the metals considered in this study, the peak-to-peak height of the Auger line was proportional to the concentration of the corresponding adsorbate.

However, the constant of proportionality is different for different adsorbates and for the same adsorbate on different metals. Meyer and Vrakking (ref. 5) showed that the Auger signal per atom of chlorine is 15.8 times that per atom of oxygen. In addition, the peak-to-peak heights in the cylindrical mirror analyzer used in this study were proportional to the peak energy (ref. 9). For chlorine relative to oxygen this introduced an additional factor of 180/510. Thus, the saturation peak-to-peak height of chlorine was divided by 5.61 for comparison with the saturation peak-to-peak height of oxygen. The saturation peak-to-peak height of oxygen on iron was arbitrarily taken to represent a concentration $c' = 1$. The saturation concentrations of oxygen and chlorine on iron and

copper were then determined to be the values shown in table I. The concentration c' is proportional to the number of atoms per unit area in the surface region.

In later measurements on the actual friction specimens, when the Auger spectrometer sensitivity was liable to change, the measured adsorbate peak-to-peak height was expressed as a fraction of the saturation peak-to-peak height as found immediately after the friction measurement. Alternatively, the Auger spectrum of the clean metal taken just before the adsorption and the spectrum of the clean metal taken just before the saturation adsorptions of table I were used to correct the spectrometer sensitivity to that of the data of table I. In either case the result was a determination of the concentration of adsorbate c' expressed as a fraction of the saturation concentration of oxygen on iron.

RESULTS

Iron and Steel

A typical friction trace for iron is shown in figure 4. Similar results were obtained for the steel specimen. Although the difference between the clean-metal curve and the curve for metal with adsorbed oxygen is small, the curves were quite reproducible, and it was not difficult to determine the static coefficient of friction by superimposing the two curves, as is done in the figure. In another series of experiments, the static coefficient of friction was measured as a function of chlorine concentration on an iron disk. The friction curves were much like those of figure 4. The results of all these tests are summarized in figure 5. The range of coefficient of friction covered in the experiments on iron and steel was limited because values above 1.5 could not be measured reliably, and the minimum coefficient observed was about 1.0.

Copper

Typical friction traces for copper with and without chlorine adsorbed are shown in figure 2. In figure 5, the results of these measurements at several chlorine coverages are shown.

Copper was also exposed to oxygen. The saturation coverage of oxygen from table I is 0.18. At this coverage the friction was indistinguishable from that of the clean metal; it was greater than 2.2. This minimum value is shown in figure 5.

Wear-Scar Features

After completion of a series of friction measurements the wear scars made by the rider on the metal disk were examined microscopically. The scars on the iron and steel disks were clearly due to multiple contact points. They were scratchy and discontinuous in the transverse direction. The scars on the copper disk were often the same, but occasionally a series of contacts would have the appearance of those in figure 6. They appear to be the result of single contact points or of multiple contact points that grew into one as the tangential force was applied.

The narrow tails on these marks were a result of lifting the rider from the disk while they were under tangential stress. The widest dimension of a mark, however, should be the width of the real area of contact. In most cases the edges of the mark were obscured by later sputter cleaning, but the widths of the marks shown in figure 6 could be measured, and they are indicated in the figure. Also indicated is the maximum coefficient of friction reached in the tests that produced each scar.

DISCUSSION

Observations

It is evident from figure 5 that the friction results for all metals tested and for all adsorbates fall on a single curve. This is even more apparent in figure 7, where the static coefficient of friction is plotted as a function of the inverse of the adsorbate coverage. The solid lines are empirically fitted to the points. The reason for the linear relation will be apparent after further analysis.

Consider first the data for iron and steel. The steel disk had a Vickers hardness about six times that of the iron disk, yet the effect of oxygen on friction was the same for both. Apparently the metal hardness was not important in these tests.

A comparison of the relative effects of chlorine and oxygen on the static friction of iron shows two things. At saturation concentration oxygen reduces the friction more than chlorine. However, this is due to the lower saturation concentration of chlorine. For it can also be seen that at equal concentrations of chlorine and oxygen the friction with chlorine will be the same as that with oxygen. This is especially apparent from figure 7. Thus, on a per-atom basis chlorine is as effective as oxygen in reducing the static friction, but the much greater saturation concentration of oxygen makes it ultimately more effective.

The results for copper with chlorine are substantially the same as those for iron. The reduction in friction per atom is identical, and since the saturation concentration

of chlorine on copper is the same as it is on iron, the minimum coefficient of static friction is the same for both, namely, about 1.0. For oxygen on copper the effect of saturation concentration is most pronounced. At saturation $c' = 0.18$ $(1/c' = 5.56)$ and $\mu_s > 2.2$. That is, the concentration is so small that no effect could be seen. It should be noticed, however, that this result is consistent with the other data.

All these observations indicate that the effect per atom of adsorbate on friction is independent of the metal substrate. That is, equal concentrations of the same adsorbate result in the same coefficient of static friction on each metal. Furthermore, chlorine and oxygen have the same effectiveness per atom in reducing friction.

Analysis

An analysis of the results in terms of the junction growth theory of friction is presented in this section. The analysis has the purposes of verifying the theory itself, finding the functional dependence of μ_s on c', and deriving a parameter related to the shear strength of the junctions that is more fundamental than the static coefficient of friction itself.

Review of theory of junction growth in clean metals. - The simple adhesion theory of the friction of metals first proposed by Bowden and Tabor (ref. 1) is based on the concept of plastic deformation of contacting asperities. Thus, when a load W is applied to a metal contact and the yield pressure of the metal is p_o, the real area of the contact is

$$A_o = \frac{W}{p_o} \tag{1}$$

Then if the specific shear strength of the metal is s_m, the tangential force required to shear the contact is

$$F = A_o s_m = \frac{W s_m}{p_o} \tag{2}$$

Since, in the absence of plowing, F is the frictional force, the coefficient of friction is

$$\mu = \frac{F}{W} = \frac{s_m}{p_o} \tag{3}$$

This theory explains the basic facts of friction, that is, that F is proportional to the load and independent of the apparent area of the contact. The theory does not, however, predict a reasonable value for μ. For most metals p_o is approximately $5s_m$. Thus, from equation (3), μ should be about 0.2. In reality values of the order of 1.0 are observed, and for atomically clean metals, μ can become as large as 50.

McFarlane and Tabor (refs. 10 and 11) expanded the junction growth theory to resolve this discrepancy. They proposed that in accordance with plasticity theory the junctions, where real metallic contact occurs, will flow plastically under the combined normal stress p and tangential stress s. The real area of contact will increase from A_o to A so that $p = W/A$ and $s = F/A$. The criterion for plastic flow by analogy with two-dimensional plasticity theory is

$$p^2 + \alpha s^2 = p_o^2 \tag{4}$$

where α is an unknown constant in the three-dimensional case. The area of contact is given by

$$\left(\frac{A}{A_o}\right)^2 = 1 + \alpha\varphi^2 \tag{5}$$

where $\varphi = F/W$ is the force coefficient.

Using equation (5) with $A_o = W/p_o$ from equation (1) gives

$$\alpha = \left(\frac{p_o A}{\varphi W}\right)^2 - \frac{1}{\varphi^2} \tag{6}$$

Note that φ is equal to the coefficient of friction when sliding occurs, if A is the largest contact area achieved.

The significance of α may be understood by considering equation (4) for very light loads, when p is nearly zero. If the tangential force is increased until plastic flow occurs, $s = s_m$ and

$$\alpha = \frac{p_o^2}{s_m^2} \tag{7}$$

Since p_o/s_m is about 5 for most metals, a value of 25 would be expected for α. Em-

pirical values of α previously measured range from 3.3 to 12. Fortunately, the results of the theory are not strongly dependent on α. A value of 9 is often chosen as approximately correct. Bowden and Tabor explain that the reason α is not actually 25 is probably that equation (4), being an extrapolation of two-dimensional plasticity theory, may not be strictly correct for the three-dimensional case.

There is excellent evidence that the theory is correct in other respects, however. McFarlane and Tabor (ref. 10) measured the real area of contact of steel balls on indium flats by determining the force of adhesion. Their results confirm equation (5), provided $\alpha = 3.3$. Using the contact resistance, Courtney-Pratt and Eisner (ref. 12) measured the area of contact of steel or platinum hemispheres of small radius on flats of like metal. Their data fit equation (6) up to the point of sliding, provided $\alpha = 12$.

In the present analysis the data of figure 8 may be used to calculate a value of α. If the diameters indicated represent the diameters of circular single junction contacts, the real area of each contact may be calculated. These areas are shown in the first column of table II. The second column shows the maximum force coefficients achieved on the corresponding friction traces.

The Vickers hardness number of the copper was 58.5±1.3 kilograms per square millimeter. If the entire real area of contact was under plastic stress, p_o was equal to 63.1±1.4 kilograms per square millimeter (ref. 13). The load W was 100 grams. Using these values in equation (6) gives the values of α listed in the third column of table II. The average of these is $\alpha = 20.9 \pm 3.0$.

A calculation of the elastic area of contact according to the Hertzian theory gives $A_e = 0.00496$ millimeter. Since this is less than the smallest area in table II, the assumption of a fully plastic junction seems reasonable. Whether or not the junction is a single circular one, as assumed, is more questionable. If the contact consists of multiple circular junctions, the method of measurement overestimates A and hence α. On the other hand, if the contact area is not circular, the value of α calculated in this study can be either too large or too small.

Considering the a priori expectation that $\alpha = 25$, the value of 20.9±3.0 found in this study, and the possible systematic errors, it seems reasonable to use 25 in the following calculations.

Review of theory of junction growth in contaminated metals. - So far, the theory does not say anything about the onset of sliding. Figure 8 shows how the friction force and shear stress increase as the real area of contact grows. While s approaches s_m asymptotically, F increases without limit. The experiments of Courtney-Pratt and Eisner verified that this behavior was correct on normally clean and lubricated metals up to the point of sliding. Tabor proposes (refs. 10 and 11) that interfacial films with a shear strength less than that of the bulk metal are the means of terminating the growth of the real area of contact.

Imagine that the shear strength of the interfacial layer is s_i. Let k be defined so that

$$s_i = ks_m \tag{8}$$

Now, since this contaminant layer is essentially two-dimensional, its yield stress is not determined by the combined normal and tangential stresses as is the yield stress for the bulk material, but is simply s_i. Thus, junction growth proceeds as long as the layer is capable of transmitting the tangential stress to the underlying metal. When the shear stress exceeds s_i, sliding begins. Tabor shows (ref. 11) that this occurs when

$$\mu_s = \frac{s_i}{p} = \frac{1}{\sqrt{\alpha}\left(k^{-2} - 1\right)^{1/2}} \tag{9}$$

where μ_s is the static coefficient of friction.

The friction traces of figure 2 exhibit this kind of behavior. When the surfaces were atomically clean, the force coefficient rose to high values with displacements of only a few micrometers more than the displacements due to yield of the system itself. With soft, clean metals the force coefficient went to well over 10 before the contact broke. With the hard metals sliding occurred at lower values. This was probably due to limitations on the growth of the junctions arising from the sphere-on-flat geometry. As the junction increased in size, further increases demanded greater amounts of plastic flow. At some point the rate of increase of the tangential force exceeded that which could be accommodated by the plastic flow in the metal and rupture occurred.

When the metals are contaminated, s_i is less than s_m, so that sliding commences at some value of force coefficient below that for the bare metal. However, when contamination is very slight, there may be no observable effect, since the geometrical factors come into play before the contaminant. This occurred, for instance, in copper with chlorine at concentrations less than 0.1 and with oxygen.

The contaminated iron and steel curves illustrated in figure 4 exhibit a rapid increase in force coefficient as soon as sliding commenced. Apparently, the interfacial layer was largely disrupted and clean metal was exposed over most of the contact area before sliding progressed past about 10 micrometers.

Whatever the reasons for the specific behavior exhibited, the value of force coefficient to be interpreted as the static coefficient of friction must be chosen carefully. For purposes of measuring the effect of contaminant coverage, the value of force coefficient at which deviation from the clean metal trace first occurs best represents the coefficient of friction μ_s in equation (9). This is the value indicated in figures 2 and 4. On the

other hand, the contact areas shown in figure 8 are the result of the highest force coefficient φ achieved during a run. This maximum value is thus the one that has been used to fit these results to equation (6).

Extension of theory of contaminated surfaces. - In order to derive a relation between the static friction and adsorbate concentration, an expression for the dependence of the interfacial shear strength s_i on the adsorbate concentration is required. The simple assumption is made that s_i varies linearly from the clean metal shear strength s_m to a value s_a when the concentration of the adsorbate is 1:

$$s_i = s_m - c(s_m - s_a) \tag{10}$$

where c is the adsorbate concentration in the junction just as yielding occurs. (A possible model corresponding to this linear theory is discussed in the next section.) From equation (8)

$$k^{-2} = \left(\frac{s_i}{s_m}\right)^{-2} = 1 - c\left(1 - \frac{s_a}{s_m}\right) \tag{11}$$

and from equation (9)

$$k^{-2} = 1 + \frac{1}{\alpha \mu_s^2} \tag{12}$$

In this analysis, the concentration c, when sliding is about to begin, is not the same as the concentration c', before the metals are placed in contact. This difference is due to the plastic flow that occurs when the tangential force is applied. However, c' is the experimentally measured quantity. Suppose that the actual amount of adsorbate in a junction does not change as the area of the junction grows. Then,

$$c = \frac{A_o}{A} c' \tag{13}$$

At the instant of sliding A is given by equation (5) with $\varphi = \mu_s$:

$$\frac{A}{A_o} = \left(1 + \alpha \mu_s^2\right)^{1/2} \tag{14}$$

The ratio A/A_o may be eliminated from equations (13) and (14) to obtain an expression for c in terms of c':

$$c = \frac{c'}{\left(1 + \alpha\mu_s^2\right)^{1/2}} \tag{15}$$

Substituting this expression into equation (11) and using equation (12) to eliminate k result in

$$1 + \frac{1}{\alpha\mu_s^2} = \left[1 - \frac{c'\left(1 - \frac{s_a}{s_m}\right)}{\sqrt{1 + \alpha\mu_s^2}}\right]^{-2} \tag{16}$$

This is a quadratic equation in μ_s. One solution implies a negative value of α and is discarded. The other is

$$\mu_s = \frac{1 - c'\left[\left(1 - \frac{s_a}{s_m}\right)\right]^2}{2\sqrt{\alpha}\, c'\left(1 - \frac{s_a}{s_m}\right)} \tag{17}$$

Equation (17) is the functional relation between μ_s and c' that was sought. To see whether this relation is consistent with the results of the friction experiments, it is noted that each pair of μ_s and c' yield one value of the quantity s_a/s_m. For any one combination of metal and adsorbate, s_a/s_m should be the same in every run. In table III the values of μ_s, c', and s_a/s_m calculated from equation (17) are listed. The agreement of the s_a/s_m values within each group is quite good. Examination of the last column also shows that the values of s_a/s_m for all the tested systems are the same within an acceptable margin of error.

While the value $\alpha = 25$ has been used in this analysis, the agreement of s_a/s_m values does not depend on the choice of α. For lower values of α, the scatter is somewhat greater. Of course, the actual values of s_a/s_m do depend on the choice of α.

The linear dependence of μ_s on $1/c'$ which is shown in figure 7 follows from

equation (17), if the approximation $\left[c'(1 - s_a/s_m)\right]^2 << 1$ is valid. Then equation (17) reduces to

$$\mu_s = \frac{1}{2\sqrt{\alpha}\left(1 - \frac{s_a}{s_m}\right)c'} \tag{18}$$

which is just the inverse of the relation required. The data in table III show that the approximation is indeed valid. The largest value of $\left[c'(1 - s_a/s_m)\right]^2$ is 0.014. Since s_a/s_m depends on the choice of α, the approximation might not be valid at smaller α. It is valid, however, for values of α greater than about 6. The solid line in figure 7 is a best fit to all the data with $s_a/s_m = 0.835 \pm 0.012$.

Provided that the value of α has been correctly chosen, the parameter s_a/s_m is fundamentally related to the effect of an adsorbate on the shear strength of a metallic interface. It is the ratio of shear strength at a concentration $c = 1$ to that of the clean metal. At any other concentration c the shear strength ratio will be s_a/s_m multiplied by c, because of the linear assumption of equation (10). The ratio s_a/s_m is apparently a property of the adsorbate only. It must be understood that the actual shear strength reduction represented by the magnitude of s_a/s_m may not be attainable for an adsorbate. First, a concentration $c = 1$ may not be attainable for the particular metal-adsorbate combination. This is particularly true since, as mentioned previously, the saturation coverage of oxygen on iron, which is taken in this analysis to be a concentration of 1, may actually correspond to a double layer of oxide rather than an adsorbed monolayer. Second, even when concentrations of 1 are attainable, the application of any tangential force will cause junction growth that results in a reduction of the concentration in accordance with equation (13). Nonetheless, saturation oxygen concentration on iron is a convenient and easily reproduced standard against which other adsorbate concentrations may be determined, and s_a/s_m is a valid measure of the effect of a particular adsorbate on the shear strength of the metallic junction.

Model for Adsorbate Effect

There are two aspects of the adsorbate effect to be considered. One is the possible mechanism by which the presence of an adsorbate atom reduces the metallic bond strength. The other is the reason for the linear relation expressed by equation (10).

With only the little information in table III available, it would be premature to propose any detailed mechanism of the effect of adsorbed species on the metallic bond. On the other hand, a very simple picture can be useful as a summary of the experimental

facts. Since the parameter that seems to characterize the effect of an adsorbate on a metal is the ratio s_a/s_m, and since this ratio is the same for all the metals tested, it appears that the effect of an adsorbate atom is to reduce the bond between metal atoms by a certain fraction. The fact that oxygen and chlorine atoms produce the same reduction in shear strength suggests that the adsorbate may simply act as a parting agent. This is, at least, the simplest picture, and it is consistent with the explanation of equation (10), which follows.

The linear dependence of the interfacial shear strength on the adsorbate concentration can be explained, if the concentration $c = 1$ corresponds to a monolayer coverage (or less). Then a fraction of the surface c is covered with adsorbate and has shear strength s_a. The uncovered area has shear strength s_m. Clearly

$$s_i = cs_a + (1 - c)s_m \tag{19}$$

Equation (19) is exactly equivalent to equation (10). This model may well describe the situation. As noted previously, however, there is a possibility that at saturation oxygen would form a double oxide layer on iron. Then the model for the linear dependence on concentration would be overly simple, but it might still apply. If for oxygen on iron the oxide rather than the chemisorbed oxygen were the effective layer for reducing the shear strength, and if the oxide were formed in such a way that its coverage were proportional to c in the range of concentrations measured in this study, the model would hold with c interpreted as the fractional area covered by oxide. The fraction of the area covered by chlorine adsorbate would be $2c$ rather than c.

The discussion of possible oxide layers must remain speculative until more data on oxygen adsorption on iron have been developed. One point should be made, however. This analysis shows that the linear hypothesis expressed in equation (10) is consistent with the static friction results. This discussion is intended to show that it is not an unreasonable model for either the oxide or chemisorbed oxygen.

CONCLUDING REMARKS

From observation of the results, certain conclusions can be drawn regarding the effect of chlorine and oxygen adsorbates on the friction of metals. With further analysis, the validity of the theory presented in this report can be checked, and from the theory further conclusions and speculations may be made.

From consideration of the experimental results we can conclued that for the systems tested in this study

(1) The static coefficient of friction decreases with increasing adsorbate concentration. It is, in fact, inversely proportional to the concentration.

(2) The static coefficient of friction is independent of the metal.

(3) For equal concentrations of adsorbate the static coefficient of friction is independent of the adsorbate.

Analysis of the results in terms of the junction growth theory permits these further conclusions:

(4) The theory agrees with the results obtained in this study. The functional relation between the static friction coefficient and the adsorbate coverage is given by equation (17) or approximately by equation (18).

(5) A value of 25 for the parameter α in the theory is consistent with contact area measurements made in this study and with theoretical expectations.

(6) The adsorbate effect is measured by the shear strength ratio s_a/s_m. This ratio is 0.835±0.012 for the systems tested.

Two assumptions are incorporated in the theory. One is the linear dependence of interfacial shear strength on adsorbate concentration expressed by equation (10). The other is the effect of junction growth on the adsorbate concentration expressed by equation (13). The success of these assumptions together with conclusions 2 and 3 suggest a simple parting agent mechanism for the effect of an adsorbate on the metallic bonds.

Finally, in regard to extreme-pressure lubrication, in a realistic lubrication situation, the role of monolayer quantities is still open to question. From the present work, however, we may conclude that monolayers can be effective in reducing metal-metal friction.

Provided that monolayers of additives are important, the quantity s_a/s_m measures only one part of the additive behavior. The other part is the concentration that exists in the real system. Because of temperature differences, mechanical effects, and the drastically different chemical environment, the concentration in a real system may bear no relation to the saturation concentration produced by exposure of a clean metal to the additive vapor at low pressure. This matter of adsorbate concentration in real systems takes on special importance in light of the adsorbate independence of s_a/s_m found in the present study.

Lewis Research Center,
National Aeronautics and Space Administration,
Cleveland, Ohio, November 11, 1974,
506-16.

REFERENCES

1. Bowden, F. P.; and Tabor, D.: Action of Extreme Pressure Lubricants. Ch. XI of The Friction and Lubrication of Solids, Vol. 2. Oxford Univ. Press (London), 1954, pp. 228-246.

2. Buckley, Donald H.: Influence of Chemisorbed Films of Various Gases on Adhesion and Friction of Tungsten. J. Appl. Phys., vol. 39, no. 9, Aug. 1968, pp. 4224-4233.

3. Bowden, Frank P.; and Tabor, David: The Friction and Lubrication of Solids. Part II. Oxford Univ. Press (London), 1964.

4. Chang, Chuan C.: Auger Electron Spectroscopy. Surface Sci., vol. 25, 1971, pp. 53-79.

5. Mayer, F.; and Vrakking, J. J.: Quantitative Aspect of Auger Electron Spectroscopy. Surface Sci., vol. 33, 1972, pp. 271-294.

6. Holloway, P. W.; and Hudson, J. B.: Kinetics of the Reaction of Oxygen with Clean Nickel Single Crystal Surfaces. I. Ni(100) Surface. Surface Sci., vol. 43, no. 1, May 1974, pp. 123-140.

7. Holloway, P. H.; and Hudson, J. B.: Kinetics of the Reaction of Oxygen with Clean Nickel Single Crystal Surfaces. II. Ni(111) Surface. Surface Sci., vol. 43, no. 1, May 1974, pp. 141-149.

8. Anderson, S.; Hammarquist, H.; and Nyberg, C.: A Low Noise X-ray Appearance Potential Spectrometer and Its Application to Chemisorption of Oxygen on Nickel. Rev. Sci. Inst., vol. 45, no. 7, July 1974, pp. 877-881.

9. Coad, J. P.; and Cunningham, J. G.: Analysis Profiles of Oxide Films on Chrome Steel by Auger Emission and X-Ray Photoelectron Spectroscopies: Electron Spectroscopy and Related Phenomena, vol. 3, 1974, pp. 435-448.

10. McFarlane, J. S.; and Tabor, D.: Relation Between Friction and Adhesion. Proc. Roy. Soc. (London), Ser. A, vol. 202, no. 1069, July 1950, pp. 244-252.

11. Tabor, D.: Junction Growth in Metallic Friction: The Role of Combined Stresses and Surface Contamination. Proc. Roy. Soc. (London), Ser. A, vol. 251, no. 1266, June 1959, pp. 378-393.

12. Courtney-Pratt, J. S.; and Eisner, E.: The Effect of a Tangential Force on the Contact of Metallic Bodies. Proc. Roy. Soc. (London), Ser. A, no. 1215, Jan. 1957, pp. 529-550.

13. Tabor, D.: The Hardness of Metals. Oxford Univ. Press, 1951, p. 98.

TABLE I. - SATURATION CONCENTRATION OF CHLORINE AND OXYGEN ON IRON AND COPPER

Substrate	Adsorbate	Concentration, c'
Iron	Oxygen	[a]1.00
	Chlorine	.68
Copper	Oxygen	0.18
	Chlorine	.65

[a]Taken as 1.00 by definition.

TABLE II. - REAL AREA OF CONTACT, MAXIMUM FORCE COEFFICIENT, AND PLASTICITY-THEORY PARAMETER CALCULATED FROM EQUATION (6) FROM DATA OF FIGURE 8

Real area of contact, A, mm^2	Maximum force coefficient, φ	Plasticity-theory parameter, α (a)
0.00785	1.0	23.5
.0133	1.8	21.1
.0177	2.6	18.1

[a]Average, 20.9±3.0.

TABLE III. - OBSERVED STATIC COEFFICIENT OF FRICTION, ADSORBATE CONCENTRATION, AND SHEAR-STRENGTH RATIO CALCULATED FROM EQUATION (17)

[Plasticity-theory parameter α, 25.]

System	Static coefficient of friction, μ_s	Adsorbate concentration, c'	Shear-strength ratio, s_a/s_m	Average s_a/s_m
Steel on iron with adsorbed chlorine	0.98	0.544	0.814	0.841±0.014
	1.08	.628	.854	
	1.14	.538	.838	
	1.16	.532	.839	
	1.25	.493	.839	
	1.36	.504	.855	
	1.50	.434	.847	
Copper on copper with adsorbed chlorine	0.97	0.648	0.842	0.843±0.005
	.98	.648	.844	
	1.24	.504	.841	
	1.28	.493	.842	
	1.50	.453	.853	
	2.16	.284	.837	
Steel on iron with adsorbed oxygen	0.61	[a]1.000	0.840	0.823±0.011
	.72	.712	.809	
	.80	.667	.815	
	.89	.600	.815	
	1.07	.556	.833	
	1.22	.467	.826	
	1.28	.445	.825	
Steel on steel with adsorbed oxygen	0.67	0.867	0.832	0.814±0.024
	.81	.600	.797	
Copper on copper with adsorbed oxygen	[b]>2.2	0.180	>0.748	>0.748

[a]Taken as 1.000 by definition.

[b]Too high for observation of adsorbate effect.

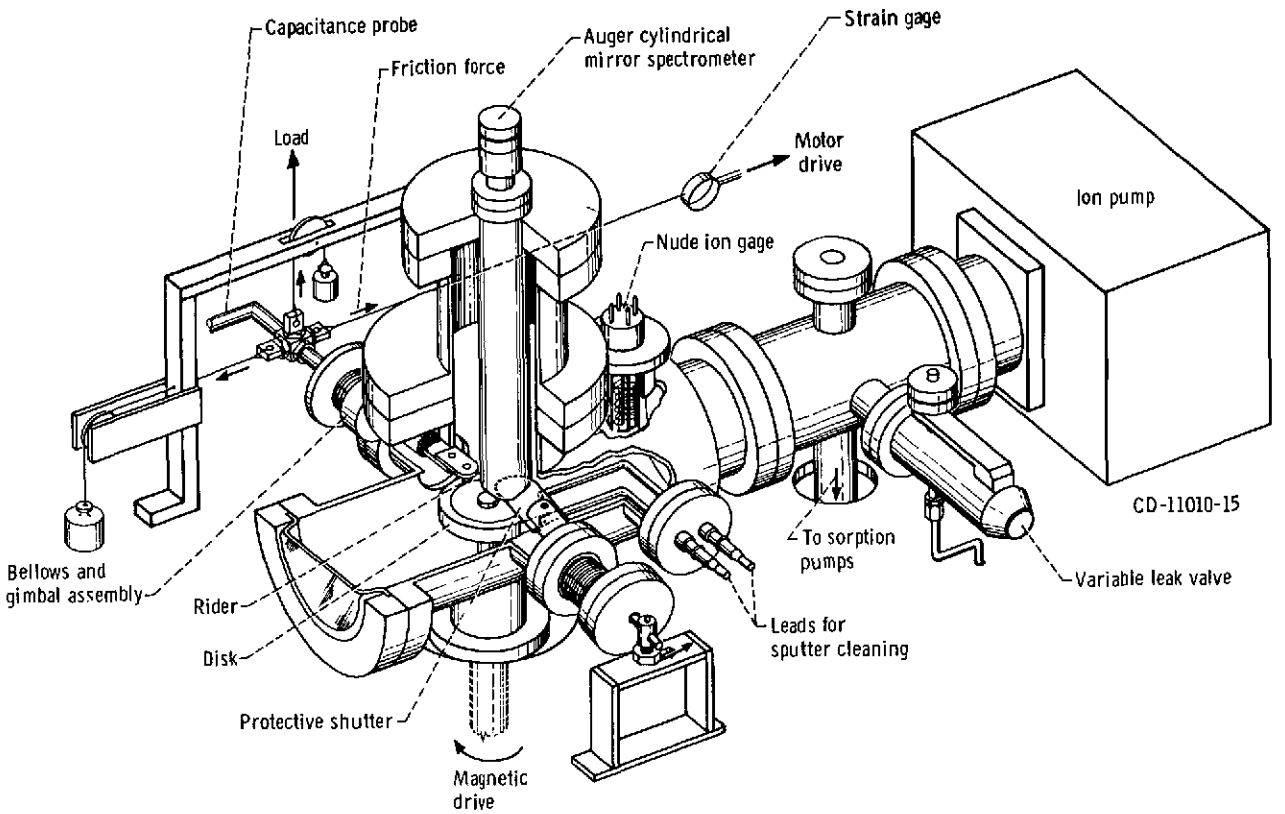

Figure 1. - Friction apparatus with Auger spectrometer.

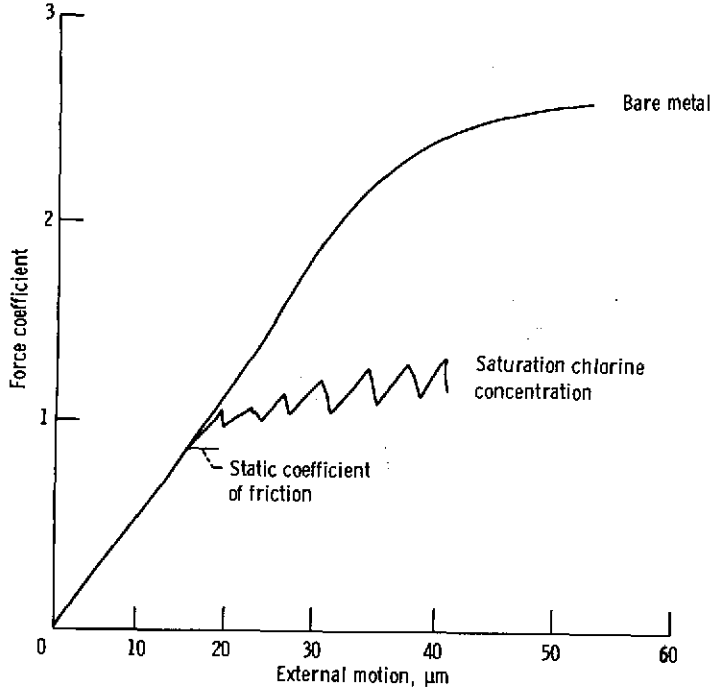

Figure 2. - Force coefficient of copper on copper with and without adsorbed chlorine as function of external motion of rider holder arm. Load, 100 grams.

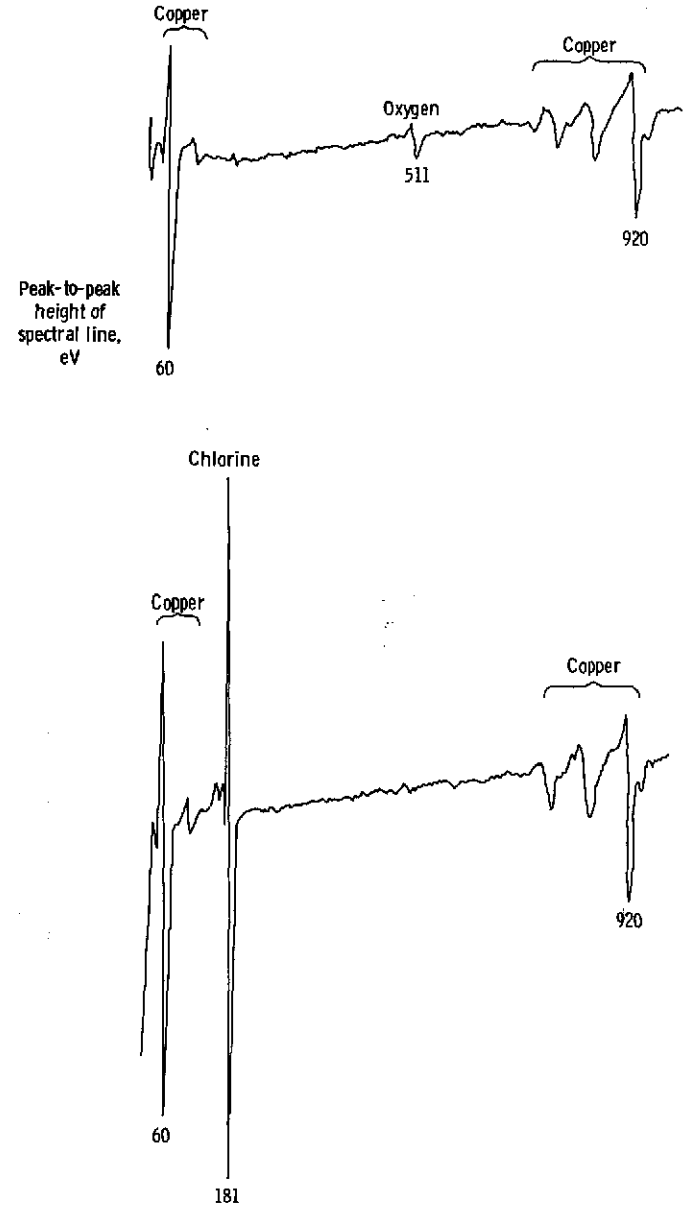

Figure 3. - Auger spectra of copper disk with saturation coverages of oxygen and chlorine.

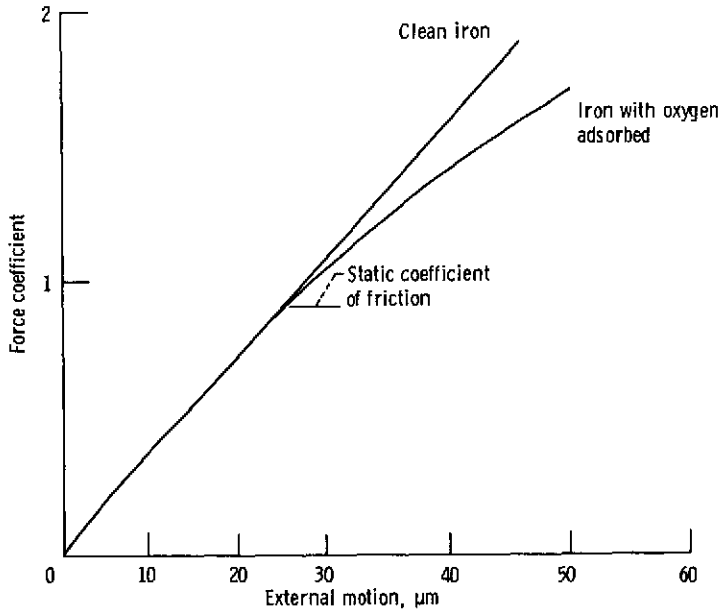

Figure 4. - Force coefficient as function of external sliding distance for iron with and without adsorbed oxygen.

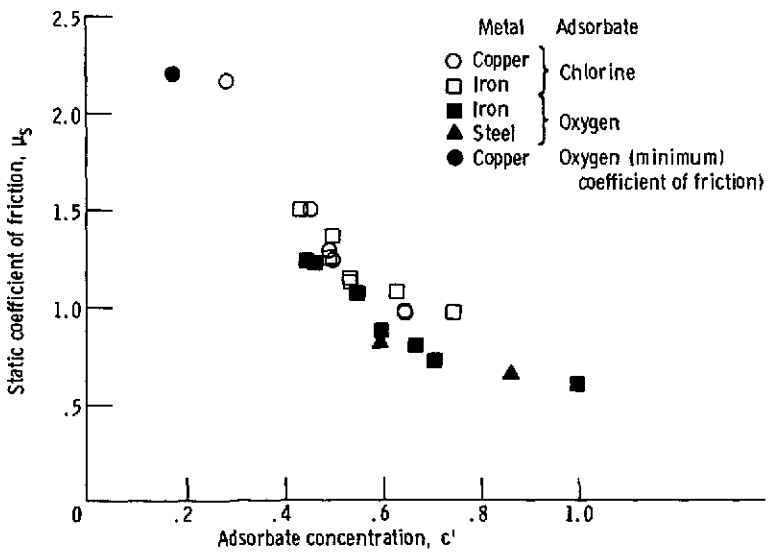

Figure 5. - Static coefficient of friction as function of adsorbate concentration.

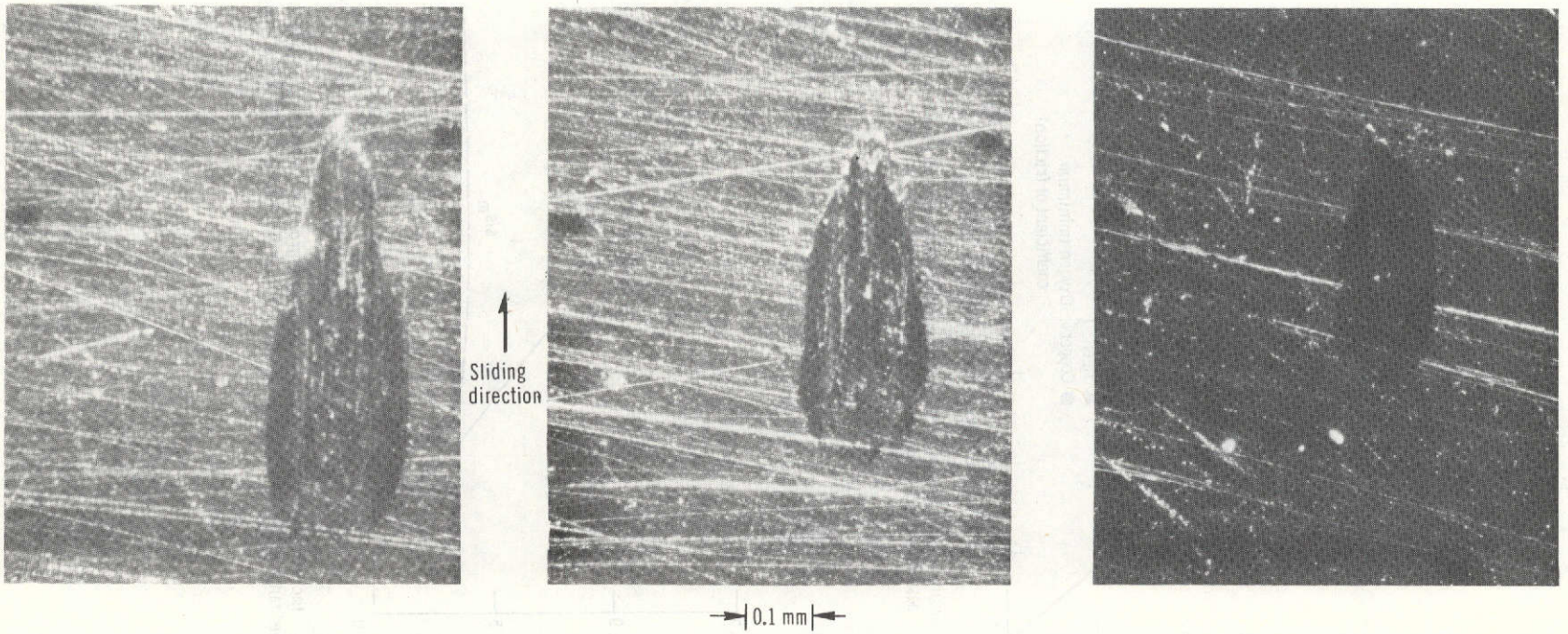

(a) Clean metal; width of wear scar, 0.15 millimeter; maximum coefficient of friction, 2.6.

(b) Intermediate coverage of chlorine; width of wear scar, 0.13 millimeter; maximum coefficient of friction, 1.8.

(c) Saturation coverage of chlorine; width of wear scar, 0.10 millimeter; maximum coefficient of friction, 1.0.

Figure 6. - Photomicrographs of abrasion on copper disk after static friction tests with transfer film of copper on steel rider.

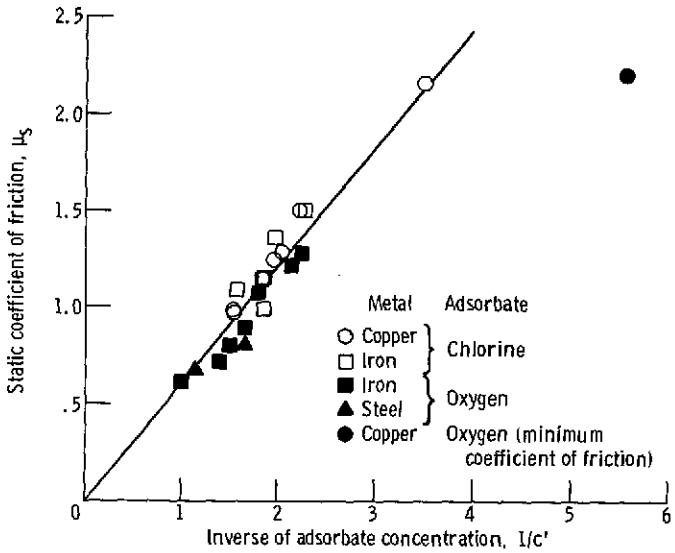

Figure 7. - Static coefficient of friction as function of inverse of adsorbate concentration.

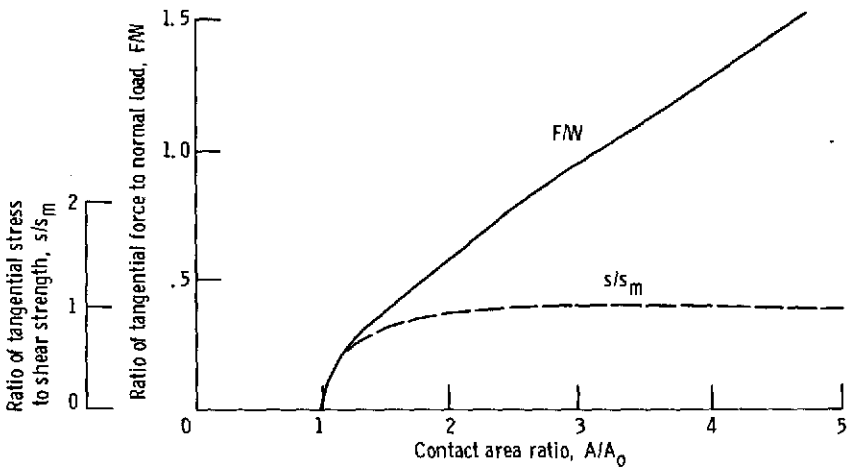

Figure 8. - Increase in tangential force and stress with growth of junction area under combined tangential force and normal force. Theory of McFarlane and Tabor (ref. 10).